Remote sensing of high temperature H2O-CO2-CO mixture with a correlated k-distribution fictitious gas method and the single-mixture gas assumption

Cyril Caliot, Yannick Le Maoult, Mouna El-Hafi, G. Flamant

Remote sensing of high temperature H_2O–CO_2–CO mixture with a correlated k-distribution fictitious gas method and the single-mixture gas assumption

C. Caliot[a,*], Y. Le Maoult[b], M. El Hafi[a], G. Flamant[c]

[a] *Laboratoire de Génie des Procédés des Solides Divisés, UMR CNRS,Ecole des Mines d'Albi Carmaux, 81 013 ALBI CT Cedex 09, France*
[b] *Centre de Recherche Outillages, Matériaux et Procédés, Ecole des Mines d'Albi Carmaux, 81 013 ALBI CT Cedex 09, France*
[c] *Laboratoire Proce´de´s, Mate´riaux et Energie Solaire, UPR CNRS, BP 5, 66125 Odeillo-Font-Romeu Cedex, France*

Abstract

Infrared spectra of high temperature H_2O–CO_2–CO mixtures are calculated using narrow band models in order to simulate hot jet signature at long distance. The correlated k-distribution with fictitious gas (CKFG) approach generally gives accurate data in such situations (especially for long atmospheric paths) but results in long computation time in cases involving mixtures of gases. This time may be reduced if the mixture is treated as a single gas (single-mixture gas assumption, SMG). Thus the lines of the single-mixture gas are assigned to the fictitious gases. In this study, the accuracy of two narrow band models is evaluated. The first narrow band model considers one single-mixture gas and no fictitious gas (CK-SMG) whereas the second model accounts for one single-mixture gas and three fictitious gases (CKFG-SMG). Both narrow band models are compared with reference spectra calculated with a line-by-line (LBL) approach. As expected, the narrow band accuracy is improved by the fictitious gas (FG) assumption particularly when long atmospheric paths are involved. Concerning the SMG assumption, it may lead to an underestimation of about 10% depending on the variation of the gas mixture composition ratio. Nevertheless, in most of realistic situations the SMG assumption results in negligible errors and may be used for remote sensing of plume signature.

Keywords: Atmospheric path; Plume signature; Remote sensing; Correlated k-distribution; Fictitious gas; Single-mixture gas

1. Introduction

Remote sensing of plume radiation involves non-homogeneous mixture containing gases and particles with high temperature gradient and large atmospheric path-lengths. Determining predictions about spectral intensity emitted from the plume requires precise absorption coefficient function integration with respect to wavenumber and distance. Accurate description of spectral absorption coefficient variations is the key problem to be solved in radiative heat transfer study involving gases. On the one hand, large number of

*Corresponding author. Tel.: +33 5 63 49 32 45; fax: +33 5 63 49 32 43.
E-mail address: cyril.caliot@enstimac.fr (C. Caliot).

spectral lines requires integration with small increments (the line-by-line (LBL) method provides necessary precision) and, on the other hand, numerical simulation of complex radiation problems in gases necessitate fast methods of computation. Then, since the LBL method is the more accurate but needs huge computer time and memory, for practical needs [1–3], the use of narrow band models leads to a more reasonable computer time. However, LBL calculations allow parameterization of approximate narrow band models and provide reliable reference calculations useful for verifying the accuracy of narrow band models. In long range sensing of plume signature, high temperature combustion gases, such as CO_2, H_2O and CO, are also present in the atmosphere. In this type of application, emission is mainly due to hot regions whereas absorption occurs principally in the cold region which is the atmosphere between hot regions and detector. In the following, we describe a computationally efficient numerical procedure for computing radiative intensities emitted by a non-homogeneous, non-isothermal column, composed of a H_2O–CO_2–CO mixture. The model allows to account for large temperature gradients and long atmospheric paths.

Among narrow band models, the correlated k-distribution approach is used. This band model approach is chosen for its numerical efficiency and its ability to include multiple scattering rigorously. But, the correlated k-distribution approach retains the relative spectral alignment of absorption lines between the hot and cold regions. In remote-sensing applications, this basic approach fails and produces large errors. This is the main limit of correlated k-distribution models. Ludwig et al. [4] have proposed to group lines on the basis of their lower-state energy value in order to improve the treatment of spectral correlations by maintaining similar behavior of each group with temperature. Rivière et al. [5] have applied this idea to the correlated k-distribution method with the so-called fictitious gases [6] which are groups of lines having similar lower-state energy values. Hereafter, the use of fictitious gases has been retained. However, another recent grouping idea has been proposed by Zhang and Modest [7] in which spectral intervals are placed into spectral groups according to their dependence on temperature and (partial) pressure. Besides, several treatments of overlapping gas mixture with the correlated k-distribution method have been proposed. One can use the multiplication property [2,3] of gases narrow band transmittivity, which implies that individual gas spectra are uncorrelated, in order to express the cumulative distribution of a mixture in terms of those of the individual gases that form the mixture [8–11]. We can also mention other contributions to the development of approximate overlapping gases treatment proposed by Gerstell [9] and Solovjov and Webb [12–14]. But, it is possible to treat overlapping bands in correlated k-distribution approach without further approximation as Goody et al. [8] notice. Then, the cumulative distribution can be formed directly from LBL mixture spectrum and the result can be treated as if the medium is described by a single complex gas.

In this paper, the LBL method used to build high resolution spectrum is detailed first. Furthermore, the narrow band model set up is presented and common problems arising with the correlated k-distribution approach combined to the fictitious gases idea and the single-mixture gas assumption are emphasized. Finally, specifically considering remote-sensing application, spectral correlations effects on narrow band radiative intensities are investigated.

2. Line-by-line model description

The monochromatic absorption coefficient of a gas mixture, at wavenumber v, is a function of gases molar fraction x_g, total pressure p, temperature T, and can be written in the form

$$\kappa_v = \sum_g \frac{x_g p}{k_B T} \sum_i S_i \Phi_i, \tag{1}$$

where k_B is the Boltzmann constant, S_i is the line intensity for the ith absorption line, of the gth gas, centered at wavenumber v_{0i},[1] and Φ_i is the Voigt line shape. The line intensity $S_i(T)$ is computed from the HITRAN [15] quantity $S_i(T_{ref})$ contained in a spectroscopic database, with the following expression:

$$S_i(T) = S_i(T_{ref}) \frac{Q(T_{ref})}{Q(T)} \exp\left[-c_2 E_i'' \left(\frac{1}{T} - \frac{1}{T_{ref}}\right)\right] \frac{1 - \exp[-c_2 v_{0i}/T]}{1 - \exp[-c_2 v_{0i}/T_{ref}]}, \tag{2}$$

[1] The collisional shift is neglected.

where T_{ref} value depends on the spectroscopic database, $Q(T)$ is the total internal partition function calculated using the parameterization of Fischer et al. [16], c_2 is the second radiation constant $c_2 = hc/k_{\mathrm{B}} = 1.4388\,\mathrm{cm\,K}$, h is the Planck constant, c the speed of light in vacuum and E_i'' is the transition lower-state energy. The spectroscopic database used for H_2O is a line list, provided by ONERA,[2] composed of lines from HITRAN [15], HITEMP [17] and from the water line list of Partridge and Schwenke [18]. For CO_2 spectroscopic database, CDSD-1000 [19] and HITEMP are publicly available. CDSD-1000 is retained since Tashkun et al. [19] have shown that CDSD-1000 is more accurate than HITEMP at temperature exceeding 1000 K. The CO spectroscopic database of HITEMP is chosen for its very high temperature validity [17]. The Voigt line shape is a good approximation near the line center

$$\Phi_i = \sqrt{\frac{\ln 2}{\pi}}\,\frac{1}{\gamma_{\mathrm{D}i}}\,\frac{y}{\pi}\int_{-\infty}^{\infty}\frac{\mathrm{e}^{-t^2}}{(x-t)^2+y^2}\,\mathrm{d}t, \tag{3}$$

Φ_i is characterized by x and y which are, respectively, the ratios $\sqrt{\ln 2}(v - v_{0i})/\gamma_{\mathrm{D}i}$ and $\sqrt{\ln 2}\gamma_{\mathrm{L}i}/\gamma_{\mathrm{D}i}$ and by the Doppler and Lorentz half-width at half-maximum (HWHM):

$$\gamma_{\mathrm{D}i} = \frac{v_{0i}}{c}\sqrt{2k_{\mathrm{B}}T\ln 2\,\frac{\mathcal{N}_{\mathrm{A}}}{M_g}}, \tag{4}$$

$$\gamma_{\mathrm{L}i} = \sum_{g'} x_{g'}\gamma^{\mathrm{s}}_{\mathrm{L},igg'}\,\frac{p}{p_{\mathrm{s}}}\left(\frac{T_{\mathrm{s}}}{T}\right)^{n_{gg'}}, \tag{5}$$

where $\mathcal{N}_{\mathrm{A}}$ is the Avogadro number, M_g the molecular weight (in $\mathrm{kg\,mol^{-1}}$), p_{s} and T_{s} are the standard pressure and temperature (1 atm, 296 K), g' is the collision partner of the absorbing molecule g, $x_{g'}$ the corresponding molar fraction, $n_{gg'}$ is a phenomenological parameter and $\gamma^{\mathrm{s}}_{\mathrm{L},igg'}$ the standard Lorentz half-width. The fast algorithm of Wells [20] is used to calculate the Voigt profile. When $n_{gg'}$ and $\gamma^{\mathrm{s}}_{\mathrm{L},igg'}$ are not included in the spectroscopic database then approximate expressions are used. Approximate expressions for H_2O line broadening by H_2O, N_2, O_2, CO_2 which are valid at high temperatures were taken from [21]. Similarly, expressions for CO_2 line broadening by CO_2, H_2O, N_2 and O_2 and expressions for CO broadening by CO_2, H_2O, N_2 and O_2 were taken, respectively, from [22] and [23]. The Voigt profile does not account neither for the finite duration of collisions nor for the line mixing effects. According to Ibgui and Hartmann [24,25], near the center of the line, line mixing effects can be disregarded since they vanish when integrated over wavenumber. However, in the line wings, the simultaneous effects of line mixing and of the finite collision duration on absorption cannot be neglected. In order to account for such effects the line profile in the wings is modified by an empirical multiplicative factor χ [26–28]. The far line wings have been corrected below 300 K, using the empirical χ functions of Clough et al. [29] for H_2O self-broadening and foreign-broadening. χ-factors used for CO_2 self-broadening, N_2 and O_2 broadening was published in [30–34]. For atmospheric temperatures, the line profile have a Lorentzian behavior and the expression of corrected profile is written in the form

$$\Phi_i = \frac{\ln 2}{\gamma^2_{\mathrm{D}i}}\,\frac{1}{\pi}\,\frac{p}{p_{\mathrm{s}}}\,\frac{\sum_{g'} x_{g'}\gamma^{\mathrm{s}}_{\mathrm{L},igg'}\left(\frac{T_{\mathrm{s}}}{T}\right)^{n_{gg'}}\chi_{gg'}}{x^2+y^2}. \tag{6}$$

The intensity and the line wing cut off adopted are, respectively, $I_{\mathrm{cut}} = 10^{-25}\,\mathrm{cm^{-2}}$ and $\Delta v_{\mathrm{cut}} = 500\,\mathrm{cm^{-1}}$. In order to improve LBL calculation efficiency, the LBL software uses a method of multiple spectral grids and line projection described by Ibgui [24,35]. This method achieves relative error lower than 0.3% on line projection and linear interpolation. The thinest grid resolution used in the multi-grid technique is fixed to $\Delta v_{hr} = 5 \times 10^{-4}\,\mathrm{cm^{-1}}$. Fig. 1 shows the validity of the LBL software. This validation is obtained comparing high-temperature high-resolution CO_2 experimental spectrum around $2271.7\,\mathrm{cm^{-1}}$ from Rosenmann et al. [36], with calculated spectrum using the LBL code. The experimental pure CO_2 transmission spectrum has been measured for the following conditions: $T = 789\,\mathrm{K}, p = 18\,\mathrm{mbar}, \ell = 11.48\,\mathrm{cm}$. Tashkun et al. [19] have obtained the same calculated spectrum.

[2]Office National d'Etudes et de Recherches Aerospatiales.

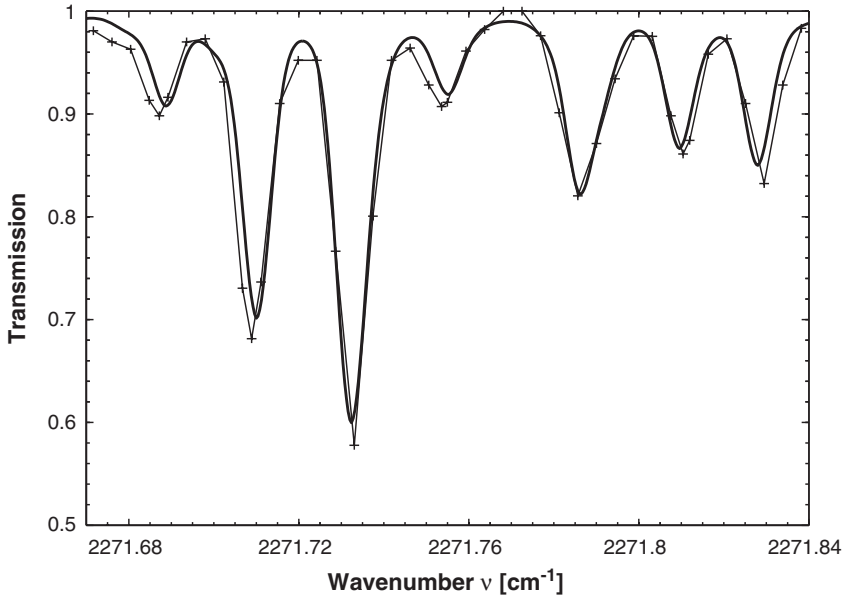

Fig. 1. CO_2 transmission spectra near 2271.75 cm^{-1}: (− + −) experimental [36]; (—) calculated. $T = 789$ K, $p = 18$ mbar, $x_{CO_2} = 1$, $\ell = 11.48$ cm.

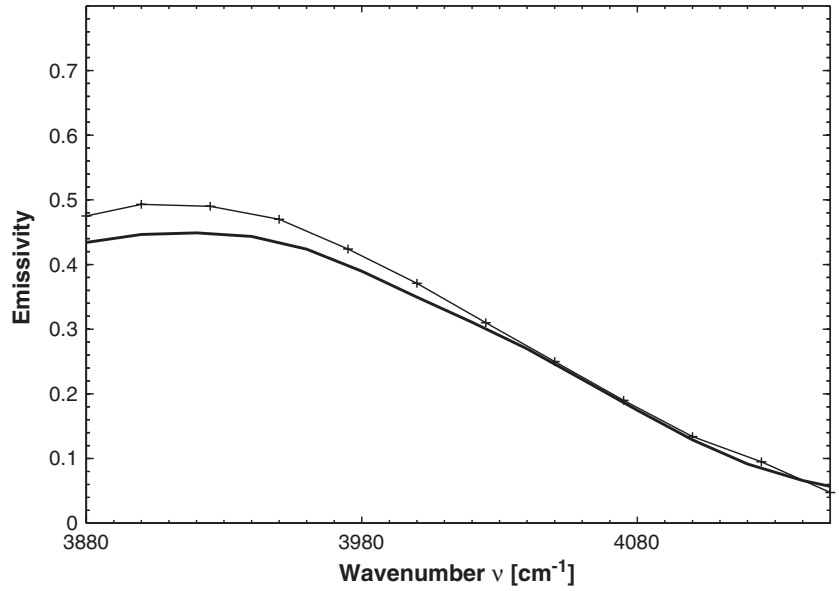

Fig. 2. H_2O emissivity spectra between 3880 and 4180 cm^{-1}: (− + −) experimental [37]; (—) calculated. $T = 1450$ K, $p = 1$ atm, $x_{H_2O} = 0.1735$, $\ell = 150$ cm.

Moreover, Fig. 2 shows computed H_2O high-temperature spectroscopic database results compared to Ludwig [37] experimental result. The experimental H_2O emissivity spectrum has been measured for the following conditions: $x_{H_2O} = 0.1735, T = 1450$ K, $p = 1$ atm, $\ell = 150$ cm. The calculated spectrum is convoluted using a triangular apparatus function of 40 cm^{-1} full-width at half-maximum [38]. Good agreement is found in the spectral range beyond 4000 cm^{-1} between the experimental spectrum of Ludwig [37] and the calculated spectrum using our LBL code and ONERA database. But, in the spectral interval between 3880 and 4000 cm^{-1} errors lower than 10% are found with the calculated spectrum which underestimates the emissivity. This error comes either from the database used where lines having high lower states energies should missed, or from experimental uncertainties on the measured spectrum.

3. Single-mixture gas and correlated-k with fictitious gases model description

The k-distribution method is used to integrate absorption coefficient κ_ν in a narrow band, $\Delta\nu$. This approach takes into account the highly repetitive character of absorption line spectrum. The computational efficiency can be improved by replacing the integration over wavenumber by an integration over the κ space [39,40], since the spectral average depends on the k-distribution but is independent of the ordering of the absorption coefficient. Then, this integration is performed with the basic idea of grouping spectral intervals according to absorption coefficient strength. For a given absorption gas mixture in homogeneous conditions under which pressure and temperature are constant, the exact spectral average of any function $I(\kappa_\nu)$ may be expressed by

$$\overline{I} = \frac{1}{\Delta\nu}\int_{\Delta\nu} I(\kappa_\nu)\,\mathrm{d}\nu = \int_0^\infty I(k)f(k)\,\mathrm{d}k, \tag{7}$$

where $f(k)$ is the absorption coefficient distribution function and $f(k)\,\mathrm{d}k$ denotes the probability that the absorption coefficient κ_ν belongs in the range k and $k+\mathrm{d}k$. Several authors [41–47] have applied the k-distribution method to radiative problems in terrestrial atmosphere. The k-distribution approach is developed for a homogeneous path and its extension to non-homogeneous path, the correlated k-distribution method (CK), was first proposed by Lacis et al. [48]. With this method, the integration over wavenumber is replaced by one over the g-space,

$$\overline{I} = \int_0^1 I(k_g)\,\mathrm{d}g = \sum_{i=1}^{N_\mathrm{q}} \omega_i I(k_{g_i}) \tag{8}$$

with, g the cumulative distribution function, a monotonically increasing function of k, which can be inverted to yield k as a function of g, is defined by

$$g(k) = \int_0^k f(k')\,\mathrm{d}k' \tag{9}$$

$g(k)$ represents the fraction of $\Delta\nu$ where κ_ν lies between 0 and k. Finally, the spectral integration is carried out with a N_q points quadrature formula (Eq. (8)), where ω_i and g_i are, respectively, quadrature weights and abscissa since the variation of I vs. g is smooth. In the CK method, the effects of profile inhomogeneities (pressure broadening, temperature) are modeled through the hypothesis that absorption coefficient spectrum is correlated over the ν-space (or g-space) at any point of a non-homogeneous path. Thus, when relative spectrum shape is not preserved, the correlated k-distribution hypothesis fails. Many authors have investigated the CK method [8,49–51]. But, for particular objectives, the only way to assess the accuracy of the CK method is to compare its results with LBL reference calculations.

In long range sensing and plume signature, large variations of temperatures exist along a line of sight and the relative strength of different spectral lines within $\Delta\nu$ change drastically with spatial position. Namely, in high temperature regions radiation is due to the so-called *hot-lines* whereas in low temperature regions these lines do not exist. Consequently, the correlation hypothesis of the CK method fails because it associates spectrum intervals where κ_ν is large in hot regions, with spectrum intervals where κ_ν is large in cold regions. It is a matter of fact that these spectrum intervals are differently located in ν-space, since the first belongs to high E'' emission lines and the later belongs to low E'' absorption lines. Then, as it can be expected, absorption due to the atmosphere is overestimated and this error tends to increase with the atmospheric path-length. Ludwig et al. [4] proposed to divide spectral lines into groups so that all lines in a particular group will have similar strengths and temperature dependencies to improve the accuracy of calculation. This similar behavior with temperature is necessary to preserve relative spectrum shape along a line of sight. This grouping is best done on the basis of the energy of the lower state of the transition E'' and all the lines belonging to one group constitute a fictitious gas [6]. The CK fictitious gas method (CKFG) was first presented by Rivière et al. [5] (see also Refs. [52,53]) for only one gas, H_2O. If the radiative transfer equation (RTE) is formulated under its differential form, correlated k-distribution method results in long computation time when applied to radiative

transfer in a mixture of N_g gases since the RTE have to be resolved $N_{\mathrm{q}}^{N_g}$ times. The CKFG approach addresses such cases.

The basic CKFG method consists in dividing one real gas in N_{fg} fictitious gases which include lines from the same $\Delta E''$ intervals. This basic CKFG method when applied to each mixture component would lead to a huge number of iterations, $N_{\mathrm{q}}^{N_g \cdot N_{fg}}$. The idea of Fu and Liou [50], who calculate CK parameters for a single-mixture gas, may be extended to decrease the total number of fictitious gases ($N_g \cdot N_{fg}$) and greatly enhance computational efficiency. Our idea is firstly to put together all the lines from every real gases in order to create a single-mixture gas (SMG approach) with its own line database. Then, we build a single gas, similar to the mixture, which has a complex spectral behavior. Secondly, we divide this single-mixture gas in N_{fg} fictitious gases with lines having their E'' in a given range $\Delta E''$. This final step applies the fictitious gas idea to lines having similar behavior with temperature to a single-mixture gas. We anticipate the additional blurring of the correlated assumption due to the variability of the real gases mixing ratio, as Fu and Liou [50] pointed out. For a non-homogeneous and isothermal column, the SMG assumption is valid if the mixing ratio of each real gas is conserved along the line of sight. Then, spectra are correlated and relative spectrum shape is preserved. Generally, mixing ratios along a line of sight are variable and this source of discrepancies is investigated in the results section.

In the following, CK and CKFG narrow band parameters of a 10-point Gauss–Legendre quadrature are determined from LBL spectra calculations with a bisection method. CK parameters are calculated taking account for the whole single-mixture gas spectrum whereas CKFG parameters are calculated for each fictitious gas of the SMG spectrum.

4. Radiative intensity methods of computation

We consider the radiative intensity $\overline{I}$ averaged on a narrow band $\Delta\nu$ and emitted from a non-homogeneous and non-isothermal column. The line of sight is discretized in N_{c} homogeneous and isothermal gaseous columns and the monochromatic radiative intensity is averaged on $\Delta\nu = 25\,\mathrm{cm}^{-1}$ in order to compare LBL results with CK single-mixture gas (CK-SMG) and CKFG-SMG results. LBL computations of monochromatic radiative intensities are carried out using the discretized integral form of the RTE:

$$I_\nu = \sum_{n=1}^{N_{\mathrm{c}}} [1 - \tau_{\nu n}] L_\nu^o(T_n) \prod_{n'=n+1}^{N_{\mathrm{c}}} \tau_{\nu n'} \tag{10}$$

with $L_\nu^o(T_n)$ the Planck function at T_n, the nth gaseous column temperature, and the monochromatic transmittivity is defined by

$$\tau_{\nu n} = \exp[-\kappa_{\nu n} \ell_n], \tag{11}$$

where κ_ν is the monochromatic absorption coefficient of the mixture and ℓ_n is the length of the column. In the CK-SMG method, the integration along the line of sight can be carried out in g-space under the correlation assumption. Then, computations are made over the full line of sight extent for each fixed value of g before being summed over N_{q} to obtain the narrow band radiative intensity

$$\overline{I} = \sum_{i=1}^{N_{\mathrm{q}}} \omega_i I(k_{g_i}). \tag{12}$$

This is the fixed-g concept which allows computation of pseudo-monochromatic radiative intensities $I(k_{g_i})$ by monochromatic formula such as

$$I(k_{g_i}) = \sum_{n=1}^{N_{\mathrm{c}}} [1 - \tau_{g_i n}] L_\nu^o(T_n) \prod_{n'=n+1}^{N_{\mathrm{c}}} \tau_{g_i n'} \tag{13}$$

with

$$\tau_{g_i n} = \exp[-k_{g_i n} \ell_n], \tag{14}$$

where $k_{g_i n}$ is the absorption coefficient of the nth column corresponding to the abscissa g_i. In the CKFG-SMG method, we follow the same procedure as in the CK-SMG method but assumption that fictitious gases

Table 1
Comparisons between RTE resolution numbers required to compute the intensities emitted in a narrow band, with $\Delta v = 25\,\mathrm{cm}^{-1}, \Delta v_{hr} = 5 \times 10^{-4}\,\mathrm{cm}^{-1}, N_g = 3, N_{fg} = 3, N_\mathrm{q} = 10$

Models	Resolution numbers
LBL	$\frac{\Delta v}{\Delta v_{hr}} = 5 \times 10^4$
Basic CKFG	$N_\mathrm{q}^{N_g \cdot N_{fg}} = 10^9$
CKFG-SMG	$N_\mathrm{q}^{N_{fg}} = 10^3$
Basic CK	$N_\mathrm{q}^{N_g} = 10^3$
CK-SMG	$N_\mathrm{q} = 10$

absorption spectra are uncorrelated is required. For improving computational efficiency, we consider here three fictitious gases since Rivière et al. [5] found similar results when using three or five fictitious gases. Many studies of Taine and co-workers [3,5,6,11,52,53] use different fictitious gas classes and hereafter, we choose the following three fictitious gases classes [5] $\Delta E''$, 0–1500 cm^{-1}, 1500–3000 cm^{-1} and 3000 $\mathrm{cm}^{-1} - \infty$. Thus, the pseudo-monochromatic radiative intensities can be written in the form

$$I(k_{g_i}, k_{g_j}, k_{g_k}) = \sum_{n=1}^{N_\mathrm{c}} [1 - \tau_{g_{ijk}n}] L_\nu^o(T_n) \prod_{n'=n+1}^{N_\mathrm{c}} \tau_{g_{ijk}n'} \tag{15}$$

with

$$\tau_{g_{ijk}n} = \exp[-(k_{g_i n} + k_{g_j n} + k_{g_k n})\ell_n] \tag{16}$$

and be summed as

$$\overline{I} = \sum_{i=1}^{N_\mathrm{q}} \sum_{j=1}^{N_\mathrm{q}} \sum_{k=1}^{N_\mathrm{q}} \omega_i \omega_j \omega_k I(k_{g_i}, k_{g_j}, k_{g_k}), \tag{17}$$

where i, j, k are subscripts, respectively, relating to a single fictitious gas class. Comparisons between resolution numbers of RTE required to compute the intensities emitted by a H_2O–CO_2–CO mixture in a narrow band for different models are given in Table 1.

5. Models results and discussion

We compare computed spectra of both CKFG-SMG and CK-SMG models with LBL reference solution. Then, we consider narrow band spectra of the radiative intensity $\overline{I}$ emitted from three different columns at atmospheric pressure. Radiative intensities spectra are shown for two spectral windows, [1200–2500 cm^{-1}] and [2800–4200 cm^{-1}]. H_2O emits in both windows, while H_2O, CO_2 and CO can overlap in the [1950–2325 cm^{-1}] window. In addition, H_2O and CO_2 overlap in the [2350–2425 cm^{-1}] and [3225–3775 cm^{-1}] windows. Moreover, H_2O and CO overlap in the [1625–1925 cm^{-1}] and [3800–4350 cm^{-1}] windows. It is important to note that the overlapping boundaries cited above account for maximum spread of mixture lines arising at high temperature. The first column depicted in Fig. 3 is isothermal and highly non-homogeneous. The non-homogeneous character of this column is chosen to evaluate the validity of the single-mixture gas assumption. Fig. 3(a) shows errors induced by the overlapping mixture of H_2O–CO_2–CO between 1950 and 2250 cm^{-1}. In a like manner, Fig. 3(b) shows errors induced by the overlapping in mixture of H_2O–CO_2 between 3450 and 3775 cm^{-1}. Although the mixing ratio of each real gas changes drastically along the line of sight, the correlated assumption according to the variability of real gases mixing ratio produces maximum relative errors lower than 10% in a narrow band. Also, we notice that CKFG-SMG gives best results than CK-SMG in Fig. 3(a) whereas both SMG models have the same accuracy in Fig. 3(b). In the spectral range between 1950 and 2250 cm^{-1} of Fig. 3(a) only hot-lines belonging to H_2O and CO_2 are present whereas both cold and hot-lines are present for CO. Thus, the CKFG-SMG model is more accurate, since the blurring due to the SMG

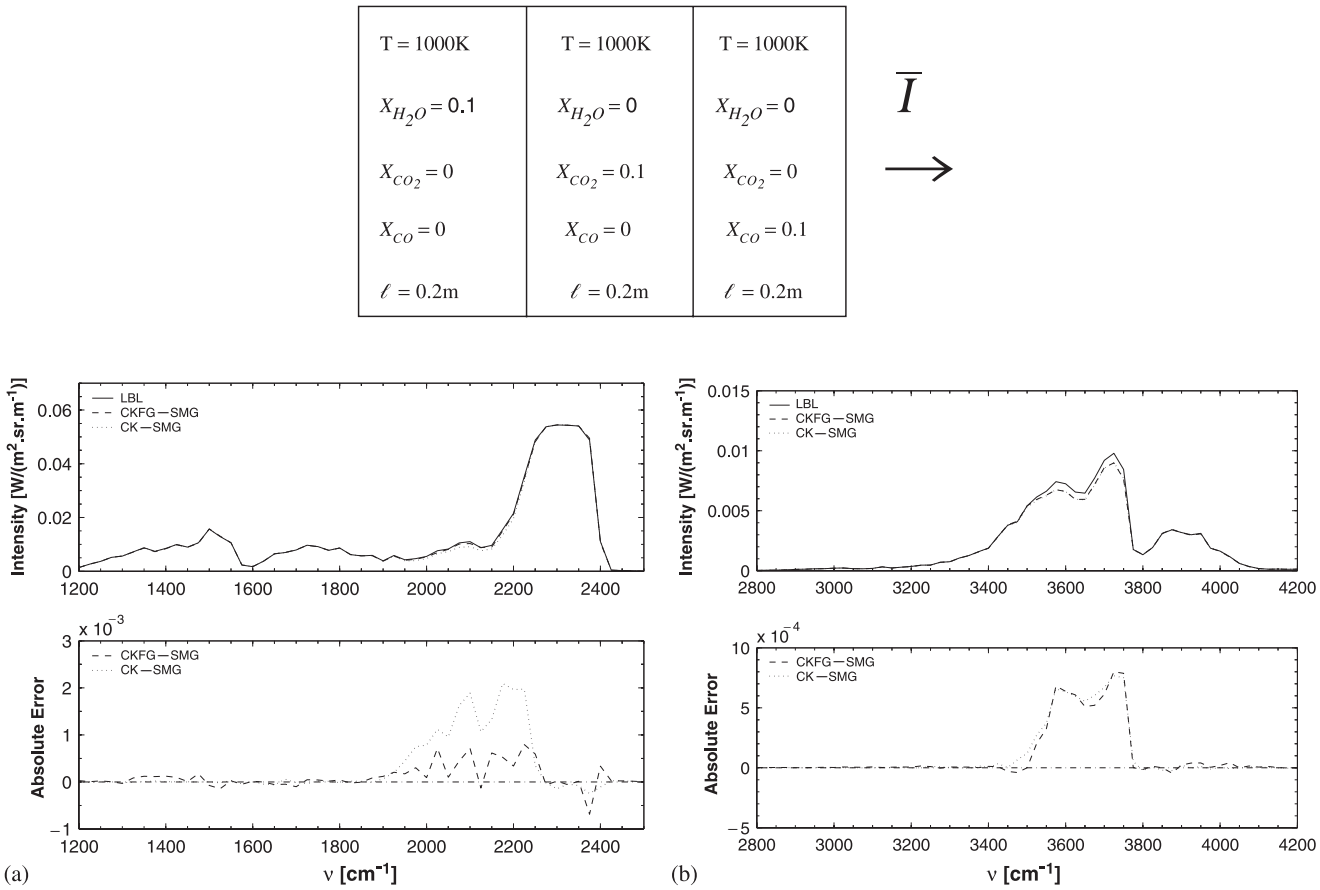

Fig. 3. Comparisons of narrow band radiative intensities spectra emitted from non-homogeneous column and computed with LBL, CKFG-SMG and CK-SMG models: (a) 1200–2500 cm^{-1}, (b) 2800–4200 cm^{-1} window.

assumption is weak for the fictitious gas which is composed of cold-lines. In the spectral range between 3450 and 3775 cm^{-1} of Fig. 3(b), H_2O and CO_2 overlapping lines are from different lower-state energies. Consequently, the blurring due to the SMG assumption affects both SMG models. The second column described in Fig. 4 is homogeneous and non-isothermal. In this case, we evaluate the efficiency of the fictitious gas assumption applied to a single-mixture gas. Fig. 4 shows the radiative intensity for the same two spectral windows as studied before in Fig. 3. In this results, two different path-lengths are involved. They correspond, respectively, to a thin and a thick optical thickness in order to represent the influence of variable atmospheric path-length. Figs. 4(a) and (c) show the radiative intensity spectra and absolute errors for a small atmospheric path-length. In both cases, CKFG-SMG gives better results than CK-SMG. For long atmospheric path, such as in Figs. 4(b) and (d), CKFG-SMG model produces a far better accuracy than CK-SMG does. Rivière et al. [5] have obtained similar results for H_2O spectra. Presently, we notice that the fictitious gas assumption gives good results for a H_2O–CO_2–CO mixture treated as a single-mixture gas. The third column shown in Fig. 5 is both non-homogeneous and non-isothermal. This column composition allows to evaluate the efficiency of both the fictitious gas and the single-mixture gas assumptions, in a quasi-realistic remote-sensing plume signature application. Fig. 5 shows the radiative intensity for two spectral windows and for two atmospheric path-lengths. In high temperature layers, mixing ratios are approximately constant. But, in the cold layer ($T = 300$ K) mixing ratios are different from their values in high temperature region. In Figs. 5(c) and (a) the influence of the cold region optical thickness is too small to produce great difference between CKFG-SMG and CK-SMG models results. For the results involving long atmospheric path-lengths in Figs. 5(b) and (d), CKFG-SMG model achieves good precision with a maximum relative error of 15% in a narrow band whereas CK-SMG model leads to a maximum error in a narrow band of more than 50%. In both Figs. 5(b) and (d), CK-SMG errors are principally due to the correlated assumption of high temperature spectrum with

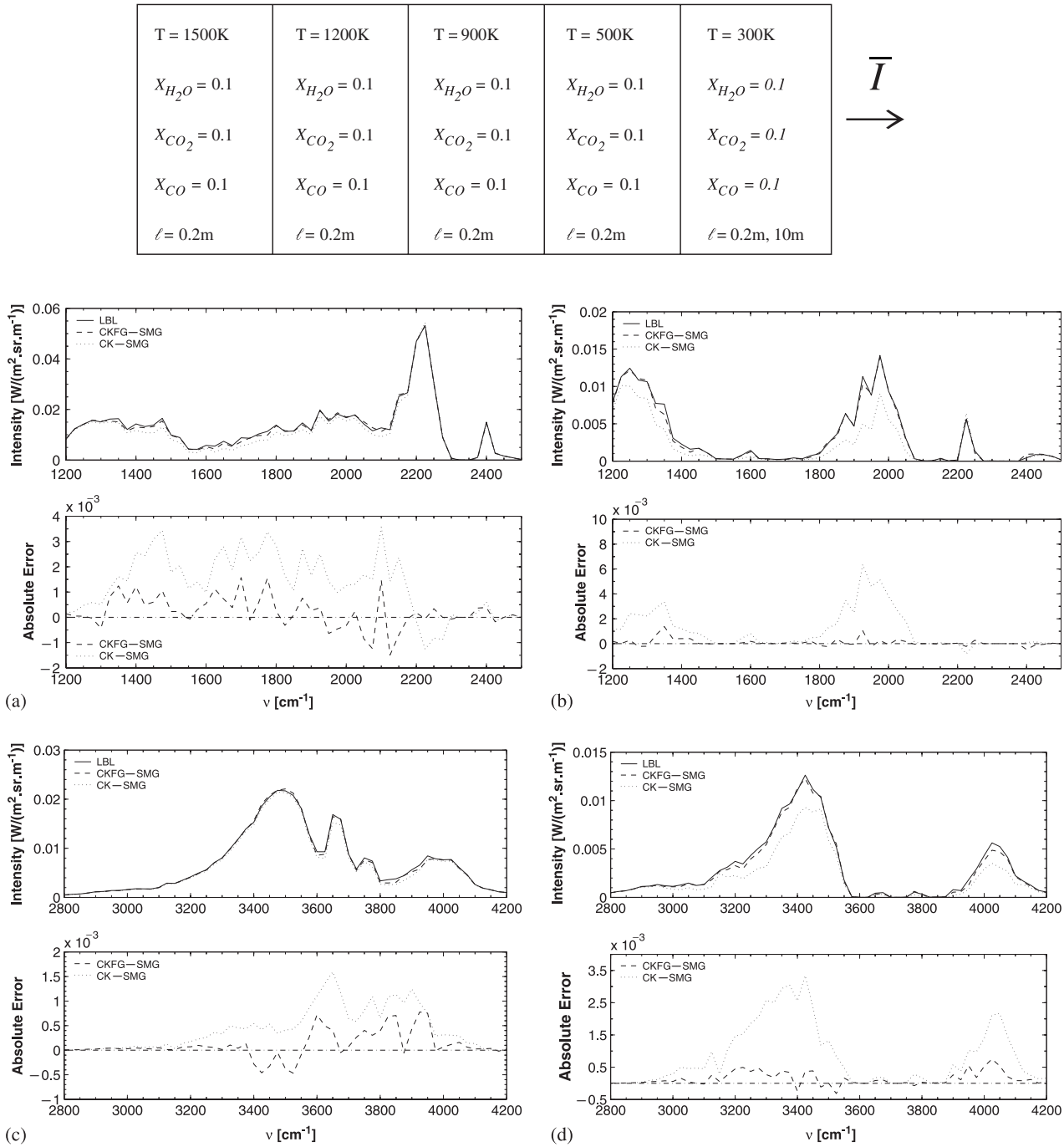

Fig. 4. Comparisons of narrow band radiative intensities spectra emitted from non-isothermal column and computed with LBL, CKFG-SMG and CK-SMG models: (a) 1200–2500 cm^{-1} and ℓ (300 K) = 0.2 m, (b) 1200–2500 cm^{-1} and ℓ (300 K) = 10 m, (c) 2800–4200 cm^{-1} and ℓ (300 K) = 0.2 m, (d) 2800–4200 cm^{-1} and ℓ (300 K) = 10 m.

atmospheric spectrum. CKFG-SMG approach which is designed for such situations is very accurate. Effects of the additional blurring due to gases mixing ratio variation are found to be negligible. In Fig. 5(b), since the CO atmospheric optical thickness is very weak, the blurring induced by the SMG assumption is due to the H_2O and CO_2 overlap in the 2100–2250 cm^{-1} spectral window. This source of discrepancies produces maximum errors in the 2100–2250 cm^{-1} spectral window lower than 15% that can be neglected especially when intensity have to be integrated on a wide spectral band. In Fig. 5(d) there is no error on intensity due to the SMG assumption since the intensity in the overlapping spectral region of H_2O and CO_2 is totally absorbed by the atmosphere. The CKFG-SMG and CK-SMG errors are principally due to spectral correlations induced

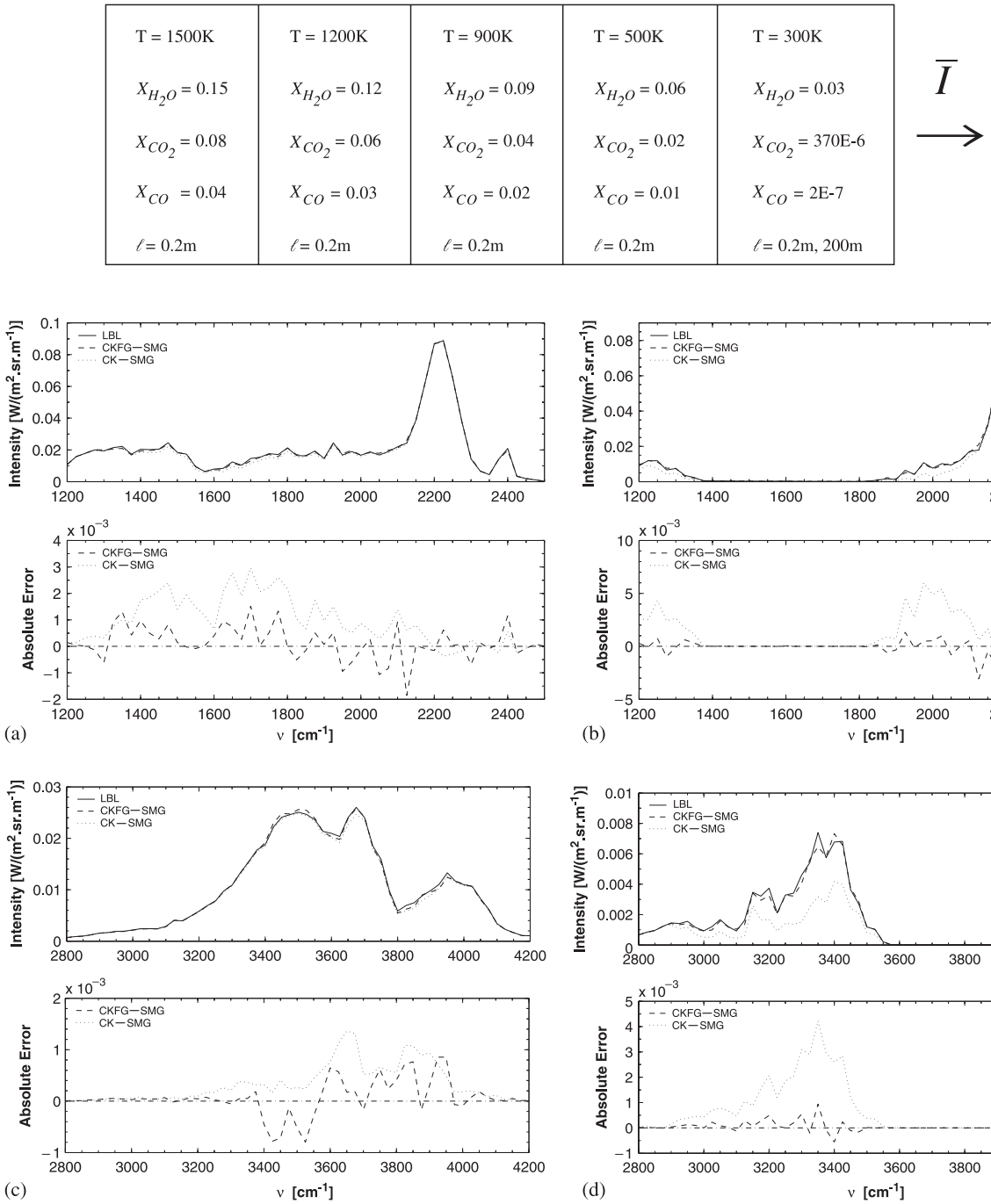

Fig. 5. Comparisons of narrow band radiative intensities spectra emitted from a non-homogeneous and non-isothermal column and computed with LBL, CKFG-SMG and CK-SMG models: (a) 1200–2500 cm^{-1} and ℓ (300 K) = 0.2 m, (b) 1200–2500 cm^{-1} and ℓ (300 K) = 200 m, (c) 2800–4200 cm^{-1} and ℓ (300 K) = 0.2 m, (d) 2800–4200 cm^{-1} and ℓ (300 K) = 200 m.

by the temperature change in column layers and long atmospheric path-length when gases mixing ratios does not change drastically in high temperature layers.

6. Conclusion

CKFG-SMG and CK-SMG models are exposed and assessed on the basis of Rivière et al. [5] work on CKFG model, and Fu and Liou [50] work with the single-mixture gas assumption (SMG). In order to improve the CK model, fictitious gases have been introduced to address strong spectral correlations due to long

atmospheric path-length. CKFG-SMG is very accurate especially when large temperature gradient and long atmospheric path are involved in comparison with CK-SMG. The single-mixture gas concept has been assumed to decrease the number of radiative transfer equation resolutions needed when treating radiatively active gases mixture. In some cases, when gases mixing ratio change along a line of sight, SMG assumption is a source of discrepancies. But, investigations of that discrepancies have shown locally relative errors lower than 10% when gases mixing ratio drastically change in the hot temperature region. In addition, SMG assumption errors can be neglected when gases mixing ratios remain approximately constant in the hot temperature region. SMG assumption allows a great reduction of gas number but shifts the computational effort into the tabulation of CK-SMG and CKFG-SMG parameters. Using single-mixture gas parameters require LBL calculations of absorption coefficient spectra at many temperatures, pressures and mixture mixing ratios. Once the tabulation is performed, simple interpolations on the database will produce precise k-distribution parameters. The tabulation of CK-SMG and CKFG-SMG parameters for H_2O–CO_2-CO mixture is now under preparation.

Acknowledgements

The authors are grateful to the Office National d'Etudes et de Recherches Aerospatiales for providing their water line list.

References

[1] Stephens GL. Review: the parameterization of radiation for numerical weather prediction and climate models. Mon Weather Rev 1984;112:826–67.
[2] Goody RM, Yung YL. Atmospheric radiation, theoretical basis. 2nd ed. New York and Oxford: Oxford University Press; 1989.
[3] Taine J, Soufiani A. Gas IR radiative properties: from spectroscopic data to approximate models. Adv Heat Transfer 1999;33:295–414.
[4] Ludwig CB, Malkmus W, Reardon JE, Thomson JAL. Handbook of infrared radiation from combustion gases. NASA SP-3080: Washington, DC, 1973.
[5] Rivière P, Soufiani A, Taine J. Correlated-k and fictitious gas methods for H_2O near 2.7 μm. JQSRT 1992;48:187–203.
[6] Levi Di Leon R, Taine J. A fictive gas-method for accurate computations of low resolution IR gas transmissivities: application to the 4.3 μm CO_2 band. Rev Phys Appl 1986;21:825–31.
[7] Zhang H, Modest MF. Scalable multi-group full-spectrum correlated-k distributions for radiative heat transfer. In: Proceedings of IMECE 2002, ASME.
[8] Goody R, West R, Chen L, Crisp D. The correlated-k method for radiation calculations in non-homogeneous atmospheres. JQSRT 1989;42:539–50.
[9] Gerstell MF. Obtaining the cumulative k-distribution of a gas mixture from those of its components. JQSRT 1993;49:15–38.
[10] Modest MF, Riazzi RJ. Assembly of full-spectrum k-distributions from a narrow-band database; effects of mixing gases, gases and nongray absorbing particles, and mixtures with nongray scatterers in nongray enclosures. JQSRT 2005;90:169–89.
[11] Pierrot L, Soufiani A, Taine J. Accuracy of narrow-band and global models for radiative transfer in H_2O, CO_2, and H_2O–CO_2 mixtures at high temperature. JQSRT 1999;62:523–48.
[12] Solovjov VP, Webb BW. SLW modeling of radiative transfer in multicomponent gas mixtures. JQSRT 2000;65:655–72.
[13] Solovjov VP, Webb BW. A local-spectrum correlated model for radiative transfer in non-uniform gas media. JQSRT 2002;73:361–73.
[14] Solovjov VP, Webb BW. The cumulative wavenumber method for modeling radiative transfer in gas mixtures with soot. JQSRT 2005;93:273–87.
[15] Rothman LS, Rinsland CP, Goldman A, Massie ST, Edwards DP, Flaud J-M, et al. The HITRAN molecular spectroscopic database and HAWKS (HITRAN atmospheric workstation): 1996 edition. JQSRT 1998; 60:665–710.
[16] Fischer J, Gamache RR, Goldman A, Rothman LS, Perrin A. Total internal partition sums for molecular species in the 2000 edition of the HITRAN database. JQSRT 2003;82:401–12.
[17] Rothman LS, Camy-Peyret C, Flaud J-M, Gamache RR, Goldman A, Goorvitch D, Hawkins RL, Schroeder J, Selby JEA, Wattson RB. HITEMP, the high-temperature molecular spectroscopic database 2000. Available through (http://www.hitran.com).
[18] Partridge H, Schwenke DW. The determination of an accurate isotope dependent potential energy surface for water from extensive ab initio calculations and experimental data. J Chem Phys 1997;106:4618–39.
[19] Tashkun SA, Perevalov VI, Teffo J-L, Bykov AD, Lavrentieva NN. CDSD-1000, the high-temperature carbon dioxide spectroscopic databank. JQSRT 2003;82:165–96.
[20] Wells RJ. Rapid approximation to the Voigt/Faddeyeva function and its derivatives. JQSRT 1999;62:29–48.
[21] Delaye C, Hartmann J-M, Taine J. Calculated tabulations of H_2O line broadening by H_2O, N_2, O_2 and CO_2 at high temperature. Appl Opt 1989;28:5080–7.

[22] Rosenmann L, Hartmann J-M, Perrin MY, Taine J. Accurate calculated tabulations of IR and Raman CO_2 line broadening by CO_2, H_2O, N_2, O_2 in the 300–2400 K temperature range. Appl Opt 1988;27:3902–7.
[23] Hartmann J-M, Rosenmann L, Perrin MY, Taine J. Accurate calculated tabulations of CO line broadening by H_2O, N_2, O_2 and CO_2 in the 200–3000 K temperature range. Appl Opt 1988;27:3063–5.
[24] Ibgui L, Hartmann J-M. An optimized line by line code for plume signature calculations-I: model and data. JQSRT 2002;75:273–95.
[25] Ibgui L, Hartmann J-M. An optimized line by line code for plume signature calculations II. Comparisons with measurements. JQSRT 2002;74:401–15.
[26] Winters BH, Silverman S, Benedict WS. Line shape in the wing beyond the band head of the 4.3 μm band of CO_2. JQSRT 1964;4:527–37.
[27] Burch DE, Gryvnak DA, Patty RR, Bartky CE. Shape of collision-broadened CO_2 lines. J Opt Soc Am 1969;59:267–80.
[28] Ma Q, Tipping RH, Boulet C, Bouanich JP. Theoretical far-wing line shape and absorption for high-temperature CO_2. Appl Opt 1999;38:599–604.
[29] Clough SA, Kneizys FX, Davies RW. Line shape and the water vapor continuum. Atmos Res 1989;23:229–41.
[30] Le Doucen R, Cousin C, Boulet C, Henry A. Temperature dependence of the absorption in the region beyond the 4.3 μm band head of CO_2. 1: pure CO_2 case. Appl Opt 1985;24:897–906.
[31] Cousin C, Le Doucen R, Boulet C, Henry A. Temperature dependence of the absorption in the region beyond the 4.3 μm band head of CO_2. 2: N_2 and O_2 broadening. Appl Opt 1985;24:3899–907.
[32] Menoux V, Le Doucen R, Boulet C. Line shape in the low frequency wing of self broadened CO_2 lines. Appl Opt 1987;26:554–62.
[33] Menoux V, Le Doucen R, Boulet C. Line shape in the low frequency wing of N_2 and O_2 broadened CO_2 lines. Appl Opt 1987;26:5183–9.
[34] Menoux V, Le Doucen R, Boissoles J, Boulet C. Line shape in the low-frequency wing of self- N_2-broadened v_3 CO_2 lines: temperature dependence of the asymmetry. Appl Opt 1991;30:281–6.
[35] Ibgui L, Etudes de spectres infrarouges pour des applications de télédétection:-développement d'un calcul raie par raie optimisé-mesures en laboratoires, sur des trajets kilométriques ou à haute température. PhD thesis, Université Paris XI, Orsay; 2000.
[36] Rosenmann L, Langlois S, Delaye C, Taine J. Diode laser measurements of CO_2 line intensities at high temperature in the 4.3 μm region. J Mol Spectrosc 1991;149:167–84.
[37] Ludwig CB. Measurements of the curves-of-growth of hot water vapor. Appl Opt 1971;10:1057–73.
[38] Rivière P, Langlois S, Soufiani A, Taine J. An approximate data base of H_2O infrared lines for high temperature applications at low resolution. Statistical narrow-band model parameters. JQSRT 1995;53:221–34.
[39] Ambartzumian V. The effect of the absorption lines on the radiative equilibrium of the outer layers of the stars. Publ Obs Astron Univ Leningrad 1936;6:7–18.
[40] Lebedinsky AI. Radiative equilibrium in the Earth's atmosphere. Proc Leningrad Univ Ser Math 1939;3:152–71.
[41] Altshuler TL, King JIF. Interference of band structures from laboratory data. Specialist conference on molecular radiation and its application to diagnostic techniques. NASA TMX 53711. National Aeronautics and Space Administration, Washington, DC, 1968. p. 96–112.
[42] Kondratyev KY. Radiation in the atmosphere. San Diego: Academic Press; 1969.
[43] Yamamoto G, Tanaka M, Asano S. Radiative transfer in water clouds in the infrared region. J Atmos Sci 1970;27:282–92.
[44] Arking A, Grossman K. The influence of line shape and band structure on temperatures in planetary atmospheres. J Atmos Sci 1972;29:937–49.
[45] Lacis AA, Hansen JE. A parameterization for the absorption of solar radiation in the Earth's atmosphere. J Atmos Sci 1974;31:118–33.
[46] Chou MD, Arking A. Computation of infrared cooling rates in the water vapor bands. J Atmos Sci 1980;37:855–67.
[47] Wang W, Shi G. Total band absorptance and k-distribution function for atmospheric gases. JQSRT 1988;39:387–97.
[48] Lacis A, Wang WC, Hansen J. Correlated k-distribution method for radiative transfer in climate models: application to effect of cirrus clouds on climate. NASA Conf Publ 1979;2076:309–14.
[49] Lacis AA, Oinas V. A description of the correlated k distribution method for modeling nongray gaseous absorption, thermal emission, and multiple scattering in vertically inhomogeneous atmospheres. J Geophys Res 1991;96:9027–63.
[50] Fu Q, Liou KN. On the correlated k-distribution method for radiative transfer in nonhomogenous atmospheres. J Atmos Sci 1992;49:2139–56.
[51] Rivière P, Scutaru D, Soufiani A, Taine J. A new ck data basis suitable from 300 K to 2500 K for spectrally correlated radiative transfer in CO_2-H_2O-transparent gaz mixtures. T. & F. Ichem, 10th international heat transfer conference, 1994. p. 129–34.
[52] Rivière P, Soufiani A, Taine J. Correlated-k fictitious gas model for H_2O infrared radiation in the Voigt regime. JQSRT 1995;53:335–46.
[53] Soufiani A, André F, Taine J. A fictitious-gas based statistical narrow-band model for IR long-range sensing of H_2O at high temperature. JQSRT 2002;73:339–47.